

Contribution from the Departments of Chemistry, The University of Texas at Austin, Austin, Texas 78712, and The University of Alabama, University, Alabama 35486

Synthesis and Structures of Di- and Trinuclear Di-*tert*-butylphosphido and Di-*tert*-butylarsenido Complexes of Iridium. X-ray Crystal Structures of $[\text{Ir}(\mu\text{-}t\text{-Bu}_2\text{E})(\text{CO})_2]_2$ (E = P, As), $[\text{Ir}(t\text{-Bu}_2\text{PH})(\text{CO})]_2(\mu\text{-H})(\mu\text{-}t\text{-Bu}_2\text{P})$, $[\text{Ir}(t\text{-Bu}_2\text{PH})(\text{CO})(\mu\text{-H})]_2(\text{H})(\mu\text{-}t\text{-Bu}_2\text{P})$, and $\text{Ir}_3(\mu\text{-}t\text{-Bu}_2\text{P})_3(\text{CO})_5$

Atta M. Arif,[†] Duane E. Heaton,[†] Richard A. Jones,^{*†} Kenneth B. Kidd,[†] Thomas C. Wright,[§] Bruce R. Whittlesey,^{||} Jerry L. Atwood,^{*†} William E. Hunter,[‡] and Hongming Zhang[‡]

Received March 3, 1987

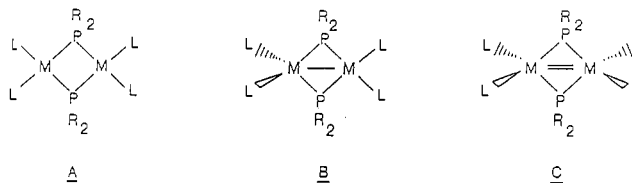
Reaction of Li-*t*-Bu₂P with $[\text{Ir}(\text{CO})_3\text{Cl}]_n$ in THF at -78 °C yields deep red $[\text{Ir}(\mu\text{-}t\text{-Bu}_2\text{P})(\text{CO})_2]_2$ (**1**) in ca. 35% yield. This complex has a planar central Ir₂P₂ core with an Ir-Ir double bond (Ir-Ir = 2.545 (1) Å). Each Ir atom bears two CO units and has a distorted tetrahedral geometry. The *t*-Bu₂As analogue of **1**, yellow $[\text{Ir}(\mu\text{-}t\text{-Bu}_2\text{As})(\text{CO})_2]_2$ (**2**), is produced in 12% yield in the reaction of $\text{Ir}_4(\text{CO})_{12}$ with *t*-Bu₂AsH in refluxing toluene. In contrast to **1**, **2** has two Ir(I) atoms that have planar coordination geometries and no Ir-Ir bond (Ir-Ir = 3.89 (1) Å). Reaction of $\text{Ir}_4(\text{CO})_{12}$ with *t*-Bu₂PH in toluene under reflux yields the dinuclear hydrido- and phosphido-bridged complex $[\text{Ir}(t\text{-Bu}_2\text{PH})(\text{CO})]_2(\mu\text{-H})(\mu\text{-}t\text{-Bu}_2\text{P})$ (**4**) (52%) as well as the trinuclear cluster $\text{Ir}_3(\mu\text{-}t\text{-Bu}_2\text{P})_3(\text{CO})_5$ (**3**) (24%). **3** consists of an Ir₃ triangle that bears one *t*-Bu₂P unit severely distorted from the Ir₃ plane and bridges two Ir atoms that bear two CO units each. The third Ir atom has only one CO group. The two other $\mu\text{-}t\text{-Bu}_2\text{P}$ units lie much closer to the Ir₃ plane. **4** has two roughly planar Ir atoms (Ir-Ir = 2.901 (1) Å) bridged by H and *t*-Bu₂P. The terminal *t*-Bu₂PH groups lie cis with respect to the Ir-Ir interaction and are trans to the $\mu\text{-}t\text{-Bu}_2\text{P}$ unit. They occupy the same side of the molecule as the $\mu\text{-H}$ atom. **4** reacts reversibly with H₂ (1 atm) in both solution and the solid state to give $[\text{Ir}(t\text{-Bu}_2\text{PH})(\text{CO})(\mu\text{-H})]_2(\mu\text{-}t\text{-Bu}_2\text{P})$ (**5**), which contains two bridging hydrides and one terminal hydride. **4** reacts with CO (1 atm) to replace one *t*-Bu₂PH ligand and give $(t\text{-Bu}_2\text{PH})(\text{CO})\text{Ir}(\mu\text{-H})(\mu\text{-}t\text{-Bu}_2\text{P})\text{Ir}(\text{CO})_2$ (**6**). The structures of **1-5** have been determined by single-crystal X-ray diffraction studies. CAD-4 crystal data: $\lambda(\text{Mo K}\alpha)$ (graphite monochromator) = 0.71073 Å. Crystal data for **1**: C₂₀H₃₆Ir₂O₄P₂, *M_r* 768.4, orthorhombic, *Pnmm* (No. 58), *a* = 8.535 (1) Å, *b* = 11.990 (1) Å, *c* = 12.574 (2) Å, *V* = 1286.8 (5) Å³, *Z* = 2, *D*_{calcd} = 2.03 g cm⁻³, $\mu(\text{Mo K}\alpha)$ = 208.7 cm⁻¹, final *R* = 0.0301 (*R_w* = 0.0382) from 954 observed (*I* > 3σ(*I*)) reflections (1331 measured). Crystal data for **2**: C₂₀H₃₆As₂Ir₂O₄, *M_r* 874.6, monoclinic, *C2/m* (No. 12), *a* = 12.009 (2) Å, *b* = 11.214 (2) Å, *c* = 11.087 (2) Å, β = 120.26 (2)°, *V* = 1289.6 (5) Å³, *Z* = 2, *D*_{calcd} = 2.25 g cm⁻³, $\mu(\text{Mo K}\alpha)$ = 128.34 cm⁻¹, final *R* = 0.0392 (*R_w* = 0.0589) from 978 observed (*I* > 3σ(*I*)) reflections (1246 measured). Crystal data for **3**: C₂₉H₅₄Ir₃O₅P₃, *M_r* 1151.6, monoclinic *P2₁/c* (No. 14), *a* = 19.753 (6) Å, *b* = 11.796 (5) Å, *c* = 17.116 (6) Å, β = 113.11 (9)°, *V* = 3668.1 (5) Å³, *Z* = 4, *D*_{calcd} = 2.01 g cm⁻³, $\mu(\text{Mo K}\alpha)$ = 112.65 cm⁻¹, final *R* = 0.039, *R_w* = 0.048 from 1782 observed reflections (*I* > 3σ(*I*)), 2701 measured. Crystal data for **4**: C₃₂H₇₁Ir₂O₂P₃, *M_r* 965.24, orthorhombic, *P2₁2₁2₁* (No. 19), *a* = 12.257 (9) Å, *b* = 15.224 (4) Å, *c* = 22.241 (8) Å, *V* = 4150.0 (5) Å³, *Z* = 4, *D*_{calcd} = 1.545 g cm⁻³, $\mu(\text{Mo K}\alpha)$ = 65.20 cm⁻¹, final *R* = 0.0713 (*R_w* = 0.0861) from 1833 observed (*I* > 3σ(*I*)) reflections (4104 measured). Crystal data for **5**: C₂₆H₆₁Ir₂O₂P₃, *M_r* 883.10, monoclinic *P2₁/c* (No. 14), *a* = 12.341 (2) Å, *b* = 12.313 (4) Å, *c* = 22.597 (9) Å, β = 92.77 (2)°, *V* = 3429.9 (5) Å³, *Z* = 4, *D*_{calcd} = 1.710 g cm⁻³, $\mu(\text{Mo K}\alpha)$ = 78.80 cm⁻¹, final *R* = 0.0592 (*R_w* = 0.0711) from 3436 observed reflections (*I* > 3σ(*I*)), 5346 measured.

Introduction

We recently described the chemistry of some di-*tert*-butylphosphido- and -arsenido-bridged (*t*-Bu₂E; E = P, As) complexes of Co and Rh as part of a study of the steric effects imparted by bulky phosphido (or arsenido) ligands in transition-metal chemistry.¹⁻⁷ For dinuclear complexes bridged by two *t*-Bu₂E groups of formula $[\text{M}(\mu\text{-}t\text{-Bu}_2\text{E})\text{L}]_2$ (M = Co(I), Rh(I); L = 2-electron donor, CO, PR₃, etc.) three different isomers have been observed (A, B, C; see Chart I). The interesting point about these isomers is that the metal-metal bond order (0, 1, or 2) and formal electron count may be correlated with the approximate coordination geometry of the metals. Thus, two square-planar, 16-electron metals have no formal bond between them (isomer A), and tetrahedral-coordinated, 18-electron metals are separated by a formal double bond (isomer C). The intermediate isomer, B, has one 18-electron (tetrahedral) metal and one 16-electron (planar) metal. For cobalt, we have so far only observed isomers of type C, i.e. those containing two roughly tetrahedral Co(I) atoms linked by a formal double Co=Co bond.² For rhodium, isomers of all three types have been isolated and characterized.³⁻⁷ It appears that the steric bulk of both the bridging and terminal groups and also the charge on the complex have an important influence on the geometries observed.

We report here studies of bulky phosphido and arsenido derivatives of iridium (Scheme I). Interestingly, for the dinuclear complexes $[\text{Ir}(\mu\text{-}t\text{-Bu}_2\text{E})(\text{CO})_2]_2$ when E = P, isomer C is the only

Chart I



M = Co, Rh, Ir

L = 2 electron donor (CO, PR₃, N₂, etc.)

product whereas when E = As isomer A is formed. The thermal reaction of *t*-Bu₂PH with $\text{Ir}_4(\text{CO})_{12}$ yields two complexes. One is the trinuclear cluster $\text{Ir}_3(\mu\text{-}t\text{-Bu}_2\text{P})_3(\text{CO})_5$ (**3**) while the other is a dinuclear hydrido bridged species $[\text{Ir}(t\text{-Bu}_2\text{PH})(\text{CO})]_2(\mu\text{-H})(\mu\text{-}t\text{-Bu}_2\text{P})$ (**4**). **4** reacts reversibly with H₂ (1 atm) to give the unsymmetrical trihydride $[\text{Ir}(t\text{-Bu}_2\text{PH})(\text{CO})(\mu\text{-H})]_2(\text{H})(\mu\text{-}t\text{-Bu}_2\text{P})$ (**5**). **4** also reacts with CO (1 atm) to give (*t*-

- (1) Jones, R. A.; Wright, T. C.; Atwood, J. L.; Hunter, W. E. *Organometallics* **1983**, *2*, 470.
- (2) Jones, R. A.; Stuart, A. L.; Atwood, J. L.; Hunter, W. E. *Organometallics* **1983**, *2*, 1437.
- (3) Jones, R. A.; Norman, N. C.; Seeberger, M. H.; Atwood, J. L.; Hunter, W. E. *Organometallics* **1983**, *2*, 1629. Kreter, P. E.; Meek, D. W. *Inorg. Chem.* **1983**, *22*, 319.
- (4) Jones, R. A.; Wright, T. C. *Organometallics* **1983**, *2*, 1842.
- (5) Gaudiello, J. G.; Wright, T. C.; Jones, R. A.; Bard, A. J. *J. Am. Chem. Soc.* **1985**, *107*, 888.
- (6) Kang, S.-K.; Albright, T. A.; Jones, R. A.; Wright, T. C. *Organometallics* **1985**, *4*, 666.
- (7) Arif, A. M.; Jones, R. A.; Seeberger, M. H.; Whittlesey, B. R.; Wright, T. C. *Inorg. Chem.* **1986**, *25*, 3943-3949.

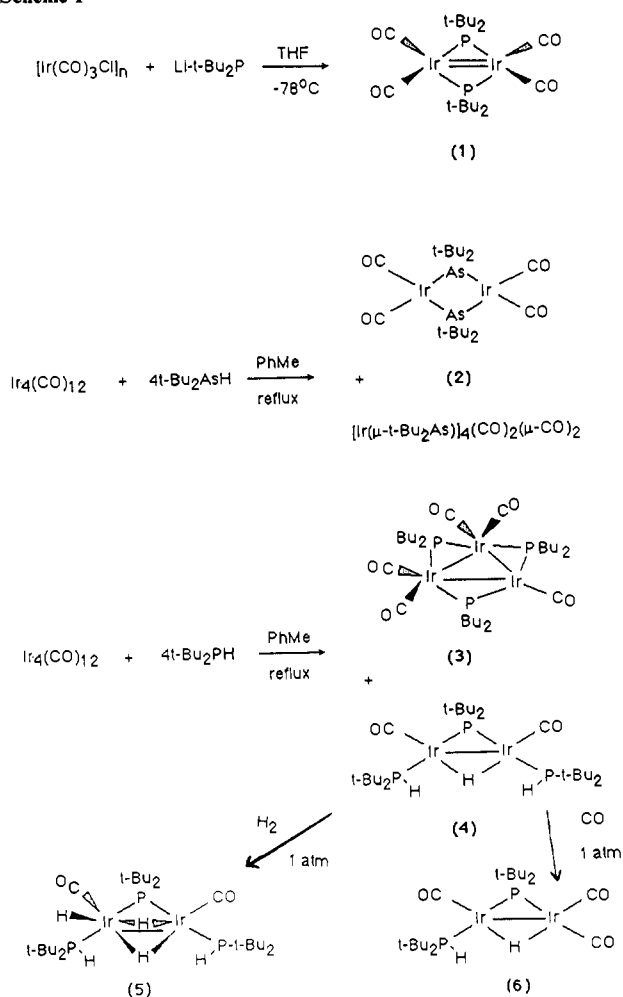
[†] The University of Texas at Austin.

[‡] The University of Alabama.

[§] Present address: Department of Chemistry, University of Texas at Arlington, Arlington, TX 76019.

^{||} Present address: Department of Chemistry, Texas Tech University, Lubbock, TX 79409.

Scheme I



$\text{Bu}_2\text{PH}(\text{CO})\text{Ir}(\mu\text{-H})(\mu\text{-}t\text{-Bu}_2\text{P})\text{Ir}(\text{CO})_2$ (6).

Few well-characterized Ir phosphido complexes have been reported. These include $[\text{Ir}(\mu\text{-PPh}_2)(\text{CO})(\text{PPh}_3)]_2$, which has a structure of type C (Chart I).⁸ Also recently reported was $\text{Ir}(\text{COD})(\mu\text{-pz})(\mu\text{-Ph}_2\text{P})_2\text{Ir}(\text{C}_8\text{H}_{13})$ (pzH = pyrazole; COD = 1,5-cyclooctadiene).⁹

This paper describes the synthesis and spectroscopic characterization of 1–6 and the X-ray crystal structures of 1–5.

Results and Discussion

Synthesis of Dimeric Complexes $[\text{Ir}(\mu\text{-}t\text{-Bu}_2\text{E})(\text{CO})_2]_2$ (E = P (1); E = As (2)). We have prepared these two complexes via different routes (Scheme I). 1 may be isolated as deep red crystals from the interaction of $[\text{Ir}(\text{CO})_3\text{Cl}]_n$ with Li-*t*-Bu₂P in THF in ca. 35% yield. 2 is formed in the reaction of *t*-Bu₂AsH with $\text{Ir}_4(\text{CO})_{12}$ (12%), which also produces the tetramer $[\text{Ir}(\mu\text{-}t\text{-Bu}_2\text{As})_4(\text{CO})_2(\mu\text{-CO})_2]$ (43%) (Scheme I). The latter complex has been described in a communication.¹⁰

Spectroscopic data for 1 and 2 are in accord with the structures as determined by X-ray crystallography. Thus, for 1, the IR spectrum has two strong bands at 1995 and 1955 cm⁻¹ while the ³¹P{¹H} NMR spectrum in C₆D₆ (ambient temperature) shows a single sharp peak shifted well downfield (δ 262.51 vs. 85%

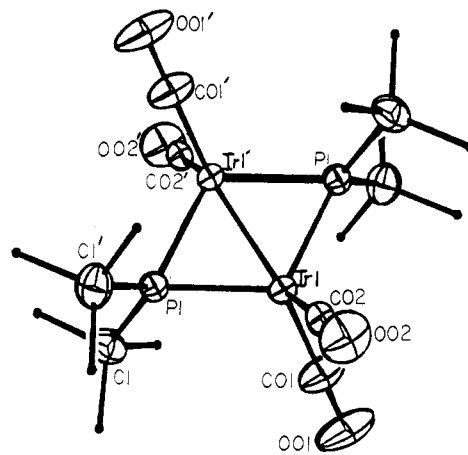


Figure 1. ORTEP drawing of 1. *t*-Bu groups have been reduced to sticks for clarity.

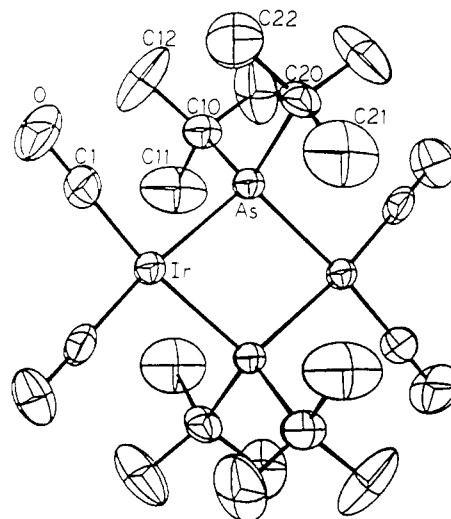


Figure 2. ORTEP drawing of 2 showing the atom-numbering scheme.

$\text{H}_3\text{PO}_4(\text{aq})$, δ 0.0) indicative of a phosphido group bridging a metal–metal bond.¹¹ For 2, the IR spectrum in the ν_{CO} region contains two strong peaks at 2010 and 1972 cm⁻¹, and the ¹H NMR spectrum consists of a single sharp peak (δ 1.44 in C₆D₆).

X-ray Structures of 1 and 2. ORTEP views of 1 and 2 are shown in Figures 1 and 2, respectively. Atomic positional parameters and bond lengths and angles are presented in Tables II and III (for 1), and IV and V (for 2). Both complexes have crystallographically imposed planar Ir₂E₂ cores.

1 has an inversion center at the midpoint of the Ir–Ir vector that is created by a mirror plane containing both Ir atoms and the CO's and containing a twofold axis, which is perpendicular to this plane and passes through the bridging phosphorus atoms. Molecules of 2 also have crystallographically imposed symmetry. In this case, the twofold axis of rotation lies along the Ir–Ir vector and the mirror plane lies perpendicular to this vector and passes through the As atoms.

The key structural difference between 1 and 2 is that (1) has tetrahedrally coordinated metals separated by an Ir=Ir double bond (isomer C) whereas 2 has metals with planar geometries and there is no Ir–Ir bond (isomer A). We have noted previously that the energy differences between these types of isomers appear to be quite small.⁶ One explanation for the differences in geometry

- (8) $[\text{Ir}(\mu\text{-PPh}_2)(\text{CO})(\text{PPh}_3)]_2$: Mason, R.; Sotofte, I.; Robinson, S. D.; Uttley, M. R. *J. Organomet. Chem.* **1972**, *46*, C61. Bellon, P. L.; Benedicenti, C.; Caglio, G.; Manassero, M. *J. Chem. Soc. Chem. Commun.* **1973**, 946. $[\text{Ir}(\mu\text{-Ph}_2\text{P})(\text{COD})]_2$: Kreter, P. E., Meek, D. W. *Inorg. Chem.* **1983**, *22*, 319.
- (9) Bushnell, G. W.; Stobart, S. R.; Vefghi, R.; Zaworotko, M. J. *J. Chem. Soc., Chem. Commun.* **1984**, 282. For heterobimetallic Ir phosphido complexes see, for example: Breen, M. J.; Shulman, P. M.; Geoffroy, G. L.; Rheingold, A. L.; Fultz, W. C. *Organometallics* **1984**, *3*, 782.
- (10) Arif, A. M.; Jones, R. A.; Schwab, S. T.; Whittlesey, B. R. *J. Am. Chem. Soc.* **1986**, *108*, 1703–1705.

- (11) Downfield shifts in the δ 50–200 range in the ³¹P NMR of the Ph₂P groups bridging metal–metal bonds have been noted by several groups of workers. See for example: Garrou, P. E. *Chem. Rev.* **1981**, *81*, 229. Carty, A. J. *Adv. Chem. Ser.* **1982**, No. 196, 163 and ref 1–5 therein. Carty, A. J.; MacLaughlin, S. A.; Nucciarone, D. In *Phosphorus-31 NMR Spectroscopy in Stereochemical Analysis*; Verkade, J. G., Quin, L. D., Eds.; VCH: 1987; Chapter 16, p 559. Similar downfield shifts have been noted for $\mu\text{-}t\text{-Bu}_2\text{P}$ complexes; see ref 1–7.

Table I. Crystal Data for Compounds 1-5

	1	2	3	4	5
Description of Crystal					
color	dark red	yellow	dark red	orange	yellow
habit	prism	plate	prism	rod	elongated prism
max cryst dimens, mm	0.10 × 0.12 × 0.15	0.05 × 0.20 × 0.25	0.08 × 0.09 × 0.10	0.10 × 0.40 × 0.80	0.35 × 0.25 × 0.20
Unit Cell					
cryst syst	orthorhombic	monoclinic	monoclinic	orthorhombic	monoclinic
space group	<i>Pnmm</i> (No. 58)	<i>C2m</i> (No. 12)	<i>P2₁/c</i> (No. 14)	<i>P2₁2₁</i> (No. 19)	<i>P2₁/c</i> (No. 14)
unit cell params					
<i>a</i> , Å	8.535 (1)	12.009 (2)	19.753 (6)	12.257 (9)	12.341 (2)
<i>b</i> , Å	11.990 (1)	11.214 (2)	11.796 (5)	15.224 (4)	12.313 (4)
<i>c</i> , Å	12.574 (2)	11.087 (2)	17.116 (6)	22.241 (8)	22.597 (9)
α , deg	90	90	90	90	90
β , deg	90	120.26 (2)	113.11 (9)	90	92.77 (2)
γ , deg	90	90	90	90	90
<i>V</i> , Å ³	1286.8 (5)	1289.6 (5)	3668.1 (5)	4150.0 (5)	3429.9 (5)
molecules/unit cell	2	2	4	4	4
formula	C ₂₀ H ₃₆ Ir ₂ O ₄ P ₂	C ₂₀ H ₃₆ As ₂ Ir ₂ O ₄	C ₂₉ H ₅₄ Ir ₃ O ₅ P ₃	C ₃₂ H ₇₁ Ir ₂ O ₂ P ₃	C ₂₆ H ₅₉ Ir ₂ O ₂ P ₃
<i>M_r</i>	786.4	874.8	1151.6	965.2	881.1
<i>d</i> _{calcd} , g cm ⁻³	2.03	2.25	2.01	1.55	1.71
μ _{calcd} , cm ⁻¹	208.7	128.3	112.7	65.2	78.8
Data Collection ^a					
scan width, deg	0.8 + 0.35(tan θ)	0.8 + 0.35(tan θ)	0.8 + 0.35(tan θ)	0.8 + 0.35(tan θ)	0.8 + 0.35(tan θ)
range of indices (<i>hkl</i>)	-10,+14,+14	+14,+12, \pm 13	+17,+10,+14	+14,+17,+25	+14,+14,+24
2 θ range, deg	2-50	2-50	2-36	2-50	3-48
no. of reflns measd	1331	1246	2701	4104	5346
std reflns (<i>hkl</i>)					
intens	181	463, 732	200	1,0,14	172, 271
orientation	533	460, 805	020, 002	656	272, 548
decay of stds	<1%	none	<2%	-5.8%	<1%
min % transmission	76.75	16.44	34.71	22.41	64.10
max % transmission	99.58	99.60	99.40	99.47	99.93
av % transmission	91.56	73.47	70.27	75.05	85.84
agreement factor for avgd reflns					
<i>F_o</i>		0.019			0.048
intens		0.034			0.086
Structure Determination					
no. of reflns used (<i>I</i> > 3 σ (<i>I</i>))	954	978	1782	1833	3436
no. of params varied	100	91	191	239	297
data/param ratio	9.54	10.75	9.33	7.67	11.57
shift to error ratio	0.03	0.029	0.010	4.138	0.275
esd of an observn of unit wt	1.257	6.933	0.990	6.560	5.884
<i>R</i> ^b	0.030	0.039	0.039	0.071	0.059
<i>R_w</i> ^c	0.038	0.059	0.048	0.086	0.071

^a For all the determinations, radiation (λ) = Mo K α (0.71073), and scan technique = $\theta/2\theta$. ^b $R = \sum |F_o| - |F_c| / \sum |F_o|$. ^c $R_w = [\sum w(|F_o| - |F_c|)^2 / \sum w |F_o|^2]^{1/2}$. The function minimized in the least squares refinement was $\sum w(|F_o| - |F_c|)^2$, $w = 1/\sigma^2(|F_o|)$.

Table II. Selected Atomic Positional Parameters for 1^a

atom	<i>x</i>	<i>y</i>	<i>z</i>	<i>B_i</i> ^b , Å ²
Ir(1)	0.42841 (4)	0.41127 (3)	0.000	1.912 (7)
P(1)	0.500	0.500	0.1622 (2)	2.12 (5)
O(O1)	0.524 (2)	0.1776 (7)	0.000	6.8 (3)
O(O2)	0.0841 (9)	0.3577 (9)	0.000	5.1 (2)
C(1)	0.338 (1)	0.5584 (7)	0.2528 (7)	3.6 (2)
C(O1)	0.485 (2)	0.2707 (9)	0.000	4.0 (3)
C(O2)	0.216 (1)	0.3766 (9)	0.000	2.8 (2)
C(11)	0.217 (1)	0.6048 (8)	0.174 (1)	5.7 (2)
C(12)	0.254 (1)	0.472 (1)	0.319 (1)	9.4 (3)
C(13)	0.395 (1)	0.642 (1)	0.328 (1)	9.3 (3)

^a Derived H atom positions are given in the supplementary material.

^b Equivalent isotropic thermal parameters defined as $\frac{1}{3}[a^2B(1,1) + b^2B(2,2) + c^2B(3,3) + ab(\cos \gamma)B(1,2) + c(\cos \beta)B(1,3) + bc(\cos \alpha)B(2,3)]$ for the anisotropically refined atoms.

is that in going from P to As in 1 to 2, there is relief of the steric congestion around the metal centers since As is bigger than P (atomic radii: P = 1.10 Å, As = 1.22 Å).¹²

Table III. Key Bond Distances (Å) and Angles (deg) for 1^a

Ir(1)-Ir(1)'	2.545 (1)	O(O1)-C(O1)	1.21 (2)
Ir(1)-P(1)	2.324 (2)	O(O2)-C(O2)	1.15 (1)
Ir(1)-C(O1)	1.83 (1)	C(1)-C(11)	1.52 (1)
Ir(1)-C(O2)	1.86 (1)	C(1)-C(12)	1.52 (2)
P(1)-C(1)	1.903 (8)	C(1)-C(13)	1.46 (1)
Ir(1)'-Ir(1)-P(1)	56.81 (3)	Ir(1)-C(O2)-O(O2)	178 (1)
Ir(1)'-Ir(1)-C(O1)	135.9 (4)	C(O1)-Ir(1)-C(O2)	91.8 (5)
Ir(1)'-Ir(1)-C(O2)	132.3 (4)	Ir(1)-P(1)-Ir(1)'	66.38 (7)
P(1)-Ir(1)-P(1)'	113.62 (7)	Ir(1)-P(1)-C(1)	118.2 (3)
P(1)-Ir(1)-C(O1)	113.2 (2)	Ir(1)-P(1)-C(1)'	118.9 (3)
P(1)-Ir(1)-C(O2)	111.6 (2)	C(1)-P(1)-C(1)'	110.4 (6)
Ir(1)-C(O1)-O(O1)	179.6 (8)		

^a Numbers in parentheses are estimated standard deviations in the least significant digits. Complete listings including C-H distances and angles involving H atoms are provided as supplementary material.²²

Several analogues of 1 are presently known. They include [Co(μ -*t*-Bu₂P)(CO)₂]₂,² [Co(μ -Ph₂P)(CO)(PET₂Ph)]₂,¹³ [Co(μ -*t*-Bu₂P)(PMe₃)L]₂ (L = CO, N₂),² [Rh(μ -*t*-Bu₂P)(CO)(PMe₃)]₂,⁴ [Rh(μ -*t*-Bu(H)P)(PMe₃)]₂,³ and [Ir(μ -Ph₂P)(CO)(PPh₃)]₂.⁸ The Ir=Ir distance in 1 (2.545 (1) Å) can be compared to that observed in [Ir(μ -Ph₂P)(CO)(PPh₃)]₂ (2.551 (1) Å) and the Ir=Ir

(12) Sutton, L. Ed *Spec. Publ.—Chem. Soc.* 1958, No. 11; 1965, No. 18. In the planar form (A), the bridging P or As atoms are closer together than in the tetrahedral form (C). This causes close hydrogen atom contacts between the *tert*-butyl groups of opposite *t*-Bu₂P units. The close contacts are reduced by going from P to As, which effectively places the *tert*-butyl groups further from each other. See ref 7 for other examples.

(13) Harley, A. D.; Whittle, R. R.; Geoffroy, G. L. *Organometallics* 1983, 2, 60.

Table IV. Atomic Positional Parameters for **2**

atom	x	y	z	$B_{eq}^a \text{ \AA}^2$
Ir	0.000	0.32635 (9)	0.000	2.71 (2)
As	0.1171 (2)	0.500	0.1543 (2)	2.51 (5)
O	0.163 (2)	0.139 (1)	0.212 (2)	7.4 (5)
C(1)	0.101 (2)	0.212 (1)	0.131 (2)	3.8 (4)
C(10)	0.101 (2)	0.500	0.330 (2)	3.9 (6)
C(11)	-0.041 (3)	0.500	0.276 (3)	9 (1)
C(12)	0.163 (2)	0.609 (2)	0.419 (2)	8.3 (7)
C(20)	0.309 (2)	0.500	0.213 (3)	3.8 (6)
C(21)	0.302 (2)	0.500	0.065 (3)	9 (1)
C(22)	0.376 (2)	0.388 (3)	0.298 (3)	8.2 (8)

^aSee footnote b in Table II.

Table V. Selected Bond Distances (Å) and Angles (deg) for **2**^a

Ir-As	2.504 (1)	C(10)-C(11)	1.49 (2)
Ir-C(1)	1.857 (7)	C(10)-C(12)	1.51 (1)
As-C(10)	2.05 (1)	C(20)-C(21)	1.60 (2)
As-C(20)	2.057 (9)	C(20)-C(22)	1.53 (1)
O-C(1)	1.170 (8)	Ir-Ir'	3.891 (1)
As-Ir-As'	77.90 (3)	As-C(10)-C(11)	104.9 (7)
As-Ir-C(1)	94.8 (2)	As-C(10)-C(12)	111.8 (6)
As-Ir-C(1)'	172.7 (2)	As-C(20)-C(21)	101.8 (7)
C(1)-Ir-C(1)'	92.5 (4)	As-C(20)-C(22)	110.4 (5)
Ir-As-Ir'	102.10 (3)	C(22)-C(20)-C(22)'	110 (1)
Ir-As-C(10)	110.0 (2)	C(11)-C(10)-C(12)	110.3 (7)
Ir-As-C(20)	111.8 (2)	C(12)-C(10)-C(12)'	108 (1)
C(10)-As-C(20)	109.1 (4)	C(21)-C(20)-C(22)	111.9 (7)
Ir-C(1)-O	179.1 (8)		

^aNumbers in parentheses are estimated standard deviations in the least significant digits.

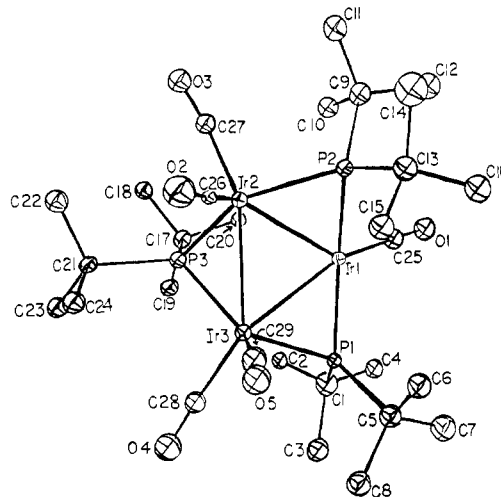
double bond found in $[\text{Ir}(\mu\text{-}t\text{-Bu}_2\text{As})_4(\text{CO})_2(\mu\text{-CO})_2]$ (2.592 (6) Å). The Ir(1)-P(1)-Ir(1)' angle of 66.38 (7)° lies in the region normally expected for a phosphido group bridging a metal-metal bond.¹⁴ The Ir(1)-P(1) distance of 2.324 (2) Å can be compared to the analogous value of 2.298 (3) Å found in $[\text{Ir}(\mu\text{-Ph}_2\text{P})(\text{CO})(\text{PPh}_3)]_2$.⁸

The structural parameters of **2** are similar to those of the rhodium analogue $[\text{Rh}(\mu\text{-}t\text{-Bu}_2\text{As})(\text{CO})_2]_2$, which we recently described.⁷ The nonbonded Ir-Ir separation of 3.89 (1) Å can be compared with a Rh-Rh value of 3.884 (1) Å in $[\text{Rh}(\mu\text{-}t\text{-Bu}_2\text{As})(\text{CO})_2]_2$ and 3.72 Å in the "A" isomer of $[\text{Rh}(\mu\text{-}t\text{-Bu}_2\text{P})(\text{CO})_2]_2$.¹ The Ir-As distance of 2.504 (1) Å in **2** is somewhat longer than analogous Ir-As distances of 2.373 (average) and 2.409 Å (average) in $[\text{Ir}(\mu\text{-}t\text{-Bu}_2\text{As})_4(\mu\text{-CO})_2(\text{CO})_2]$. The Ir-As-Ir' angle of 102.10 (3)° is typical for a diorganarsenide bridging a nonbonded interaction and is similar to the Rh-As-Rh' angle of 102.15 (2)° found in $[\text{Rh}(\mu\text{-}t\text{-Bu}_2\text{As})(\text{CO})_2]_2$.

Reaction of $\text{Ir}_4(\text{CO})_{12}$ with $t\text{-Bu}_2\text{PH}$. Preparation of $[\text{Ir}(t\text{-Bu}_2\text{PH})(\text{CO})_2(\mu\text{-H})(\mu\text{-}t\text{-Bu}_2\text{P})]$ (4**) and $\text{Ir}_3(\mu\text{-}t\text{-Bu}_2\text{P})_3(\text{CO})_5$ (**3**).** Reaction of $\text{Ir}_4(\text{CO})_{12}$ with excess $t\text{-Bu}_2\text{PH}$ in refluxing toluene yields a deep red solution from which two complexes may be isolated. They are dark red-purple $\text{Ir}_3(\mu\text{-}t\text{-Bu}_2\text{P})_3(\text{CO})_5$ (**3**) and orange $[\text{Ir}(t\text{-Bu}_2\text{PH})(\text{CO})_2(\mu\text{-H})(\mu\text{-}t\text{-Bu}_2\text{P})]$ (**4**). We recently described the Rh analogue of **4**, and it has a similar structure.⁷

Spectroscopic data for **3** are in accord with the structure as determined by X-ray diffraction (see below). Thus, the IR spectrum shows only terminal ν_{CO} absorptions, while the $^{31}\text{P}\{^1\text{H}\}$ NMR spectrum at ambient temperature consists of two broad singlets at δ 306.0 and 184.0 (relative areas 2:1). The peaks sharpen on cooling, and at -25 °C in toluene- d_6 , a doublet-triplet pattern is observed (δ 304.9 (d) and 184.0 (t), $^2J_{\text{P-P}} = 72$ Hz). The data suggest a flexing of the Ir_3P_3 framework of **3** that is rapid on the NMR time scale at ambient temperature and is slowed down upon cooling.

X-ray Structure of $\text{Ir}_3(\mu\text{-}t\text{-Bu}_2\text{P})_3(\text{CO})_5$ (3**).** Although a large number of crystals were examined, very few were of sufficient quality or size for X-ray studies. We finally obtained one crystal

**Figure 3.** ORTEP drawing of **3** showing the atom-numbering scheme.**Table VI.** Atomic Positional Parameters for **3**

atom	x/a	y/b	z/c	$U_{eq}^a \text{ \AA}^2$
Ir(1)	0.80199 (7)	0.1364 (1)	0.22089 (8)	0.030
Ir(2)	0.66776 (6)	0.1025 (1)	0.23512 (8)	0.029
Ir(3)	0.76291 (7)	0.2796 (1)	0.32135 (8)	0.029
P(1)	0.8742 (4)	0.2780 (7)	0.3023 (5)	0.029
P(2)	0.7431 (4)	-0.0332 (7)	0.2098 (5)	0.034
P(3)	0.6428 (7)	0.2980 (7)	0.2143 (5)	0.037
C(1)	0.899 (2)	0.413 (3)	0.254 (2)	0.052
C(2)	0.942 (2)	0.370 (3)	0.196 (2)	0.059
C(3)	0.938 (2)	0.502 (3)	0.319 (2)	0.071
C(4)	0.828 (2)	0.460 (3)	0.188 (2)	0.058
C(5)	0.960 (2)	0.239 (3)	0.398 (2)	0.048
C(6)	0.952 (2)	0.118 (3)	0.424 (2)	0.063
C(7)	1.031 (2)	0.238 (3)	0.377 (2)	0.068
C(8)	0.972 (2)	0.318 (3)	0.474 (2)	0.060
C(9)	0.702 (2)	-0.107 (3)	0.103 (2)	0.056
C(10)	0.634 (2)	-0.185 (3)	0.091 (2)	0.067
C(11)	0.672 (2)	-0.015 (3)	0.031 (2)	0.064
C(12)	0.761 (2)	-0.179 (3)	0.088 (3)	0.085
C(13)	0.793 (2)	-0.142 (3)	0.300 (2)	0.057
C(14)	0.809 (2)	-0.089 (3)	0.382 (2)	0.051
C(15)	0.871 (2)	-0.166 (3)	0.289 (2)	0.076
C(16)	0.751 (2)	-0.250 (3)	0.285 (3)	0.086
C(17)	0.621 (2)	0.360 (3)	0.107 (2)	0.046
C(18)	0.662 (2)	0.294 (2)	0.063 (2)	0.037
C(19)	0.535 (2)	0.347 (3)	0.045 (2)	0.052
C(20)	0.639 (2)	0.491 (3)	0.111 (2)	0.053
C(21)	0.570 (2)	0.350 (3)	0.261 (2)	0.046
C(22)	0.598 (2)	0.323 (3)	0.353 (2)	0.047
C(23)	0.498 (2)	0.287 (3)	0.214 (2)	0.055
C(24)	0.561 (2)	0.482 (3)	0.248 (2)	0.064
C(25)	0.849 (2)	0.099 (3)	0.153 (2)	0.070
C(26)	0.652 (2)	0.045 (3)	0.327 (2)	0.048
C(27)	0.579 (2)	0.068 (3)	0.145 (2)	0.042
C(28)	0.789 (2)	0.211 (3)	0.418 (2)	0.043
C(29)	0.768 (2)	0.425 (3)	0.368 (2)	0.060
O(1)	0.877 (1)	0.084 (2)	0.106 (2)	0.089
O(2)	0.636 (1)	0.010 (2)	0.382 (2)	0.071
O(3)	0.521 (1)	0.047 (2)	0.094 (1)	0.064
O(4)	0.800 (1)	0.162 (2)	0.486 (1)	0.052
O(5)	0.772 (1)	0.514 (2)	0.399 (2)	0.085

^aSee footnote b in Table II.

that was sufficient for data collection but did not give enough strong reflections for full anisotropic refinement of all non-hydrogen atoms. The Ir and P atoms were therefore refined anisotropically while the C and O atoms were refined isotropically. A view of the molecule is shown in Figure 3. Positional parameters and bond lengths and angles are given in Tables VI and VII, respectively. The structure consists of an Ir_3 triangle in which the Ir-Ir distances are indicative of single metal-metal bonds (Ir(1)-Ir(2) = 2.785 (2) Å, Ir(1)-Ir(3) = 2.729 (2) Å, Ir(2)-Ir(3) = 2.812 (2) Å). Each Ir-Ir bond is bridged by a $t\text{-Bu}_2\text{P}$ group.

(14) Billig, E.; Jamerson, J. D.; Pruett, R. L. *J. Organomet. Chem.* **1980**, *192*, C49.

Table VII. Key Bond Distances (Å) and Angles (deg) for 3^a

Ir(1)–Ir(2)	2.785 (2)	Ir(1)–Ir(3)	2.729 (2)
Ir(1)–P(1)	2.282 (8)	Ir(1)–P(2)	2.284 (8)
Ir(1)–C(25)	1.80 (4)	Ir(1)–O(1)	2.95 (3)
Ir(2)–Ir(3)	2.812 (2)	Ir(2)–P(2)	2.338 (8)
Ir(2)–P(3)	2.558 (8)	Ir(2)–C(26)	1.84 (3)
Ir(2)–C(27)	1.87 (3)	Ir(3)–P(1)	2.346 (7)
Ir(3)–P(3)	2.371 (8)	Ir(3)–C(28)	1.73 (3)
Ir(3)–C(29)	1.87 (4)	Ir(3)–O(4)	2.96 (2)
P(1)–C(1)	1.94 (3)	P(1)–C(5)	1.89 (3)
P(2)–C(9)	1.90 (3)	P(2)–C(13)	1.95 (3)
P(3)–C(17)	1.87 (3)	P(3)–C(21)	1.99 (3)
Ir(2)–Ir(1)–P(1)	116.2 (2)	Ir(3)–Ir(1)–P(1)	55.0 (2)
Ir(2)–Ir(1)–Ir(3)	61.31 (4)	Ir(2)–Ir(1)–P(2)	53.8 (2)
Ir(3)–Ir(1)–P(2)	109.5 (2)	P(1)–Ir(1)–P(2)	150.2 (3)
Ir(2)–Ir(1)–C(1)	140.5 (5)	Ir(3)–Ir(1)–O(1)	152.7 (5)
P(1)–Ir(1)–C(1)	101.7 (5)	P(2)–Ir(1)–O(1)	97.6 (6)
Ir(3)–Ir(1)–C(25)	155 (1)	Ir(2)–Ir(1)–C(25)	140 (1)
P(2)–Ir(1)–C(25)	96 (1)	P(1)–Ir(1)–C(25)	103 (1)
Ir(1)–Ir(2)–P(2)	52.1 (2)	Ir(1)–Ir(2)–Ir(3)	58.35 (4)
Ir(1)–Ir(2)–P(3)	89.7 (2)	Ir(3)–Ir(2)–P(2)	105.2 (2)
P(2)–Ir(2)–P(3)	138.7 (3)	Ir(3)–Ir(2)–P(3)	53.7 (2)
Ir(3)–Ir(2)–C(26)	97 (1)	Ir(1)–Ir(2)–C(26)	127.5 (9)
P(3)–Ir(2)–C(26)	113 (1)	P(2)–Ir(2)–C(26)	104 (1)
Ir(3)–Ir(2)–C(27)	144.3 (9)	Ir(1)–Ir(2)–C(27)	124.9 (9)
P(3)–Ir(2)–C(27)	91.0 (9)	P(2)–Ir(2)–C(27)	98.8 (9)
Ir(1)–Ir(3)–P(1)	60.33 (4)	C(26)–Ir(2)–C(27)	102 (1)
Ir(2)–Ir(3)–P(1)	113.0 (2)	Ir(1)–Ir(3)–P(1)	52.8 (2)
Ir(2)–Ir(3)–P(3)	53.3 (2)	Ir(1)–Ir(3)–P(3)	90.8 (2)
Ir(1)–Ir(3)–O(4)	106.4 (4)	P(1)–Ir(3)–P(3)	127.0 (3)
P(1)–Ir(3)–O(4)	103.4 (4)	Ir(2)–Ir(3)–O(4)	90.8 (4)
Ir(1)–Ir(3)–C(28)	105 (1)	P(3)–Ir(3)–O(4)	125.2 (5)
P(1)–Ir(3)–C(28)	101 (1)	C(29)–Ir(3)–O(4)	94 (1)
Ir(1)–Ir(3)–C(29)	148 (1)	Ir(2)–Ir(3)–C(28)	93 (1)
P(1)–Ir(3)–C(29)	100 (1)	P(3)–Ir(3)–C(28)	128 (1)
C(28)–Ir(3)–C(29)	94 (1)	Ir(2)–Ir(3)–C(29)	145 (1)
Ir(1)–P(1)–C(1)	123 (1)	P(3)–Ir(3)–C(29)	97 (1)
Ir(1)–P(1)–C(5)	119 (1)	Ir(1)–P(1)–Ir(3)	72.3 (2)
C(1)–P(1)–C(5)	108 (1)	Ir(3)–P(1)–C(1)	117 (1)
Ir(1)–P(2)–C(9)	120 (1)	Ir(3)–P(1)–C(5)	117 (1)
Ir(1)–P(2)–C(13)	115 (1)	Ir(1)–P(2)–Ir(2)	74.1 (2)
C(9)–P(2)–C(13)	111 (1)	Ir(2)–P(2)–C(9)	116 (1)
Ir(2)–P(3)–C(17)	119 (1)	Ir(2)–P(2)–C(13)	118 (1)
Ir(2)–P(3)–C(21)	113 (1)	Ir(2)–P(3)–Ir(3)	73.0 (2)
C(17)–P(3)–C(21)	110 (1)	Ir(3)–P(3)–C(17)	125 (1)
Ir(2)–C(26)–O(2)	174 (3)	Ir(3)–P(3)–C(21)	112 (1)
Ir(3)–C(28)–O(4)	173 (3)		
Ir(1)–C(25)–O(1)	174 (3)		
Ir(2)–C(27)–O(3)	174 (3)		
Ir(3)–C(29)–O(5)	179 (3)		

^a A complete listing is provided in the supplementary material.²²

Two Ir atoms (Ir(2) and Ir(3)), each bear two CO ligands while the third (Ir(1)) has only one. There is a dramatic distortion of the unique *t*-Bu₂P group (P(3)) that bridges Ir(2) and Ir(3), giving rise to a dihedral angle of 116.4° between the P(3)–Ir(2)–Ir(3) plane and the Ir₃ plane. The other two *μ*-*t*-Bu₂P groups are both distorted out of the plane but by different amounts. The dihedral angle between the planes P(2)–Ir(1)–Ir(2) and Ir₃ is 29.3° while that between P(1)–Ir(3)–Ir(1) and Ir₃ is only 4.0°. To our knowledge, there have been no other iridium analogues of **3** reported although a number of trinuclear Rh–diphenylphosphido-bridged complexes have been reported. Haines and English have recently reported extensive studies on the trinuclear Rh–Ph₂P⁻-bridged system based on [Rh(*μ*-Ph₂P)(CO)₃]₃ and its derivatives.^{14,15} In some respects, the structure of **3** is similar to the structures of Rh₃(*μ*-Ph₂P)₃(CO)₅ and Rh₃(*μ*-Ph₂P)₃(CO)₃(PPh₃)₂, which have the general structure shown in Figure 4. In these complexes, the phosphido bridge is greatly distorted from the Rh₃ plane and spans two Rh atoms that each bear two two-electron donors (CO or PPh₃). The remaining Rh bears only one

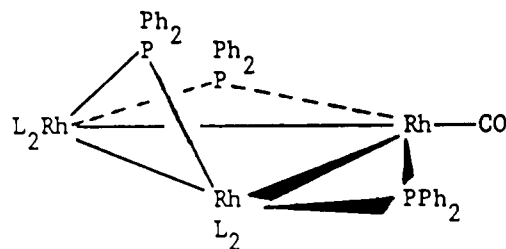


Figure 4. General structure of Rh₃(*μ*-Ph₂P)₃(CO)₅ and Rh₃(*μ*-Ph₂P)₃(CO)₃(PPh₃)₂.^{14,15}

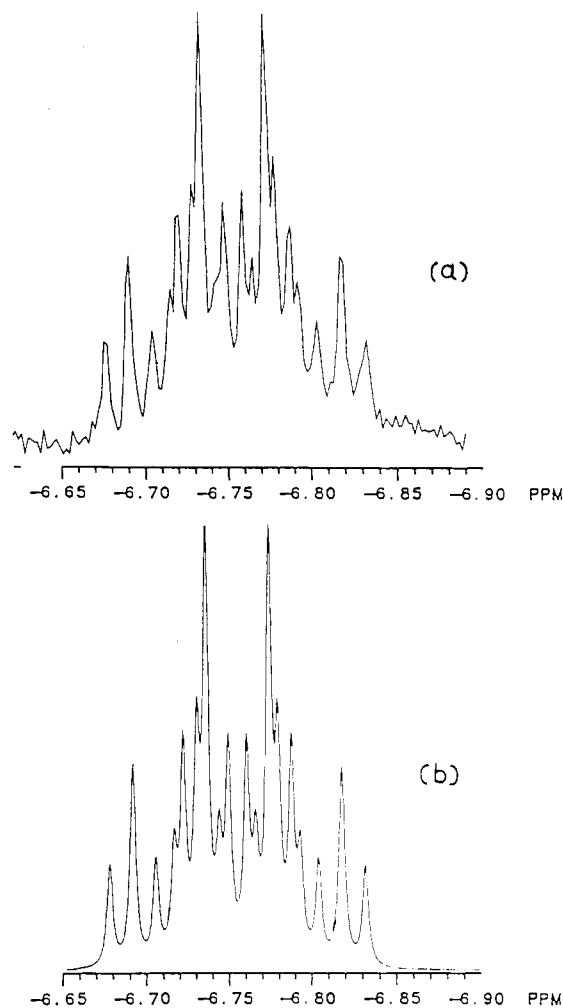


Figure 5. Observed (a) and simulated (b) ¹H NMR spectra for the bridging hydride resonance in **4**. Conditions: (a) toluene-*d*₈, ambient temperature at 361.084 MHz, acquisition time 1.45 s, pulse width 9.00 μs (90°); (b) δ(*μ*-H) –6.755, ³J_{H(1)–H(2)}} = ³J_{H(1)–H(3)}} = 4.95 Hz, ²J_{H(1)–P(1)}} = J_{H(1)–P(2)}} = 15.84 Hz, J_{H(1)–P(3)}} = 13.86 Hz, where P(1), P(2), and P(3) are as in Figure 6, H(1) is the bridging hydride, and H(2) and H(3) are the two P–H hydrogen atoms attached to P(1) and P(2), respectively.

CO ligand and can be considered coordinatively unsaturated with a 16-electron count. Of related interest is the *t*-Bu₂P⁻ analogue of **3** Rh₃(*μ*-*t*-Bu₂P)₃(*μ*-CO)(CO)₄, which has a distinctly different structure despite the same stoichiometry.¹⁶ The reasons for these differences in geometry are not immediately obvious to us.

[Ir(*t*-Bu₂PH)(CO)]₂(*μ*-H)(*μ*-*t*-Bu₂P) (**4**). Crystals of **4** rapidly lose crystallinity in the absence of solvent, and this hampered our X-ray diffraction studies. However, NMR and IR spectroscopic data are in good agreement with the X-ray structure, which is of sufficient quality to provide key structural information. The IR spectrum shows only terminal ν_{CO} absorptions in addition to a weak ν_{P–H} stretch at 2295 cm⁻¹, confirming the presence of the

(15) Haines, R. J.; Steen, N. D. C. T.; English, R. B. *J. Chem. Soc., Dalton Trans.* 1984, 515.

(16) Jones, R. A.; Wright, T. C. *Inorg. Chem.* 1986, 25, 4058.

Table VIII. Atomic Positional Parameters for **4**

atom	x	y	z	$B, \text{\AA}^2$
Ir(1)	0.1455 (2)	0.0531 (2)	0.7356 (1)	4.97 (4)
Ir(2)	0.3081 (2)	0.1369 (2)	0.6601 (1)	4.33 (4)
P(1)	-0.033 (1)	0.070 (2)	0.699 (1)	11.6 (7)
P(2)	0.237 (1)	0.213 (1)	0.5775 (8)	6.2 (4)
P(3)	0.3305 (9)	0.0586 (9)	0.7479 (6)	4.8 (3)
O(1)	0.097 (3)	-0.048 (3)	0.845 (2)	10 (1)
O(2)	0.554 (4)	0.151 (5)	0.630 (3)	36 (2)
C(1)	0.118 (5)	0.009 (4)	0.799 (3)	9 (2) ^b
C(2)	0.488 (7)	0.161 (6)	0.635 (4)	16 (3) ^b
C(10) ^c	0.359	0.312	1.027	
C(20) ^c	0.750	0.187	0.986	
C(30) ^c	0.668	0.207	0.945	
C(40) ^c	0.639	0.291	0.984	
C(50) ^c	0.527	0.291	1.000	
C(60) ^c	0.555	0.332	1.055	
C(110)	-0.115 (5)	0.148 (4)	0.746 (3)	8 (2) ^b
C(111)	-0.237 (5)	0.165 (5)	0.704 (3)	12 (2)
C(112)	-0.078 (6)	0.234 (5)	0.758 (4)	15 (2) ^b
C(120)	-0.078 (6)	-0.010 (5)	0.619 (4)	9 (2) ^b
C(121)	-0.201 (9)	-0.021 (7)	0.625 (5)	17 (4) ^b
C(122)	-0.024 (6)	-0.085 (5)	0.638 (3)	16 (2) ^b
C(210)	0.262 (4)	0.342 (4)	0.582 (3)	6 (1) ^b
C(211)	0.189 (5)	0.386 (4)	0.530 (3)	10 (2)
C(212)	0.198 (7)	0.362 (6)	0.641 (4)	12 (2) ^b
C(213)	0.385 (5)	0.363 (5)	0.566 (6)	19 (4)
C(220)	0.269 (5)	0.158 (4)	0.507 (3)	8 (2) ^b
C(221)	0.205 (6)	0.199 (5)	0.459 (3)	11 (2)
C(222)	0.233 (9)	0.072 (5)	0.512 (4)	16 (3)
C(223)	0.381 (4)	0.177 (6)	0.492 (3)	13 (3)
C(310)	0.377 (4)	0.121 (3)	0.816 (2)	6 (1) ^b
C(311)	0.498 (5)	0.152 (4)	0.808 (3)	9 (2)
C(312)	0.324 (4)	0.204 (3)	0.813 (2)	6 (1) ^b
C(313)	0.351 (7)	0.077 (5)	0.877 (3)	12 (2)
C(320)	0.398 (4)	-0.060 (4)	0.737 (3)	6 (1) ^b
C(321)	0.347 (5)	-0.091 (3)	0.678 (2)	6 (1)
C(322)	0.373 (5)	-0.116 (4)	0.798 (3)	9 (2)
C(323)	0.526 (4)	-0.042 (4)	0.721 (4)	13 (2)

^aSee Footnote *b* in Table II. ^b*B* values for isotropically refined atoms. ^cC(10)–C(60) are the carbon atoms of the hexane of crystallization. They were given fixed coordinates and isotropic thermal parameters of 6.0.

t-Bu₂PH ligands. The ³¹P{¹H} NMR spectrum is a straightforward doublet–triplet pattern consistent with a μ -*t*-Bu₂P unit coupled to two equivalent phosphine *t*-Bu₂PH groups. (δ 193.8 (t), 44.6 (d), ²*J*_{PP} = 183 Hz). In addition, the ¹H NMR spectrum contains peaks for the *t*-Bu₂PH protons (δ 5.24 (d, ¹*J*_{P-H} = 322 Hz)) and the μ -H atom (δ -6.78 (m)). We have successfully simulated this signal (Figure 5). A good agreement between simulated and experimental spectra was achieved when the μ -H unit was allowed to couple to all three phosphorous nuclei as well as the *t*-Bu₂PH protons.

X-ray Crystal Structure of [Ir(*t*-Bu₂PH)(CO)]₂(μ -H)(μ -*t*-Bu₂P) (4**).** As noted above, our X-ray studies were hampered by poor crystal quality due mainly to solvent dependency and also their platelike nature. The latter caused an acute absorption correction problem. In the absence of solvent, the crystals rapidly crumble and lose crystallinity. Although many crystals were examined, only one was of sufficient quality to give a data set and this was less than perfect. On refinement, two of the methyl carbon atoms of the *t*-Bu group on P(1) could not be located. (See Experimental Section). We have included our X-ray studies on **4** in this paper since they provide some fundamental chemical information concerning the overall molecular framework of the compound.

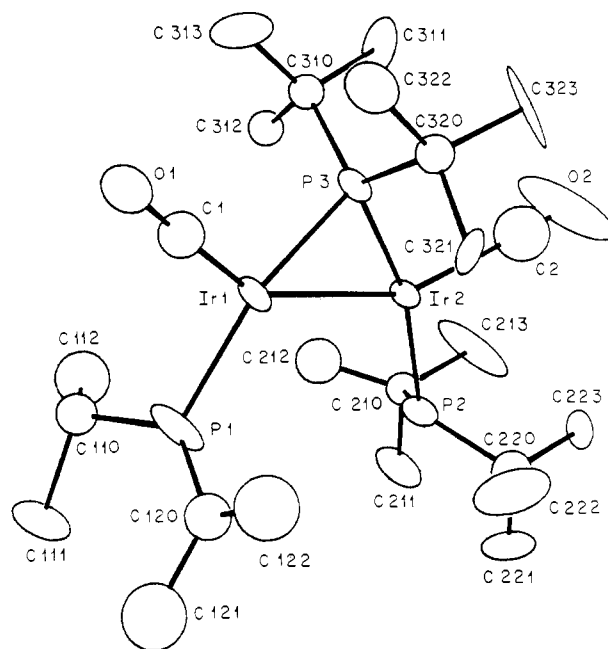
4 crystallizes the monoclinic space group *P*2₁2₁2₁ with four molecules in the unit cell. Positional parameters and bond lengths and angles are given in Tables VIII and IX, respectively. A view of the molecule is shown in Figure 6.

The overall structure of **4** consists of two distorted-square-planar Ir(I) atoms bridged by one *t*-Bu₂P group and an H atom. Although the hydride was not located in the structure, the geometry of the molecule indicates that it occupies a bridging position between the two Ir atoms. The Ir–Ir distance of 2.901 (1) Å is

Table IX. Key Bond Distances (Å) and Angles (deg) for **4**^a

Ir(1)–Ir(2)	2.901 (1)	P(1)–C(120)	1.74 (4)
Ir(1)–P(1)	2.342 (7)	P(2)–C(210)	1.98 (2)
Ir(1)–P(3)	2.285 (4)	P(2)–C(220)	1.82 (3)
Ir(1)–C(1)	1.60 (3)	P(3)–C(310)	1.88 (2)
Ir(2)–P(2)	2.346 (7)	P(3)–C(320)	2.00 (2)
Ir(2)–P(3)	2.303 (5)	O(1)–C(1)	1.37 (3)
Ir(2)–C(2)	2.30 (4)	O(2)–C(2)	0.83 (4)
P(1)–C(110)	1.88 (3)		
Ir(2)–Ir(1)–P(1)	113.2 (3)	Ir(1)–P(1)–C(120)	116 (1)
Ir(2)–Ir(1)–P(3)	51.0 (1)	C(110)–P(1)–C(120)	129 (1)
Ir(2)–Ir(1)–C(1)	147 (1)	Ir(2)–P(2)–C(210)	113.0 (8)
P(1)–Ir(1)–P(3)	164.2 (3)	Ir(2)–P(2)–C(220)	111.3 (9)
P(1)–Ir(1)–C(1)	99 (1)	C(210)–P(2)–C(220)	118 (1)
P(3)–Ir(1)–C(1)	97 (1)	Ir(1)–P(3)–Ir(2)	78.4 (2)
Ir(1)–Ir(2)–P(2)	114.5 (2)	Ir(1)–P(3)–C(310)	114.4 (7)
Ir(1)–Ir(2)–P(3)	50.5 (1)	Ir(1)–P(3)–C(320)	111.2 (6)
Ir(1)–Ir(2)–C(2)	150 (1)	Ir(2)–P(3)–C(310)	117.4 (7)
P(2)–Ir(2)–P(3)	164.9 (2)	Ir(2)–P(3)–C(320)	114.7 (7)
P(2)–Ir(2)–C(2)	95 (1)	C(310)–P(3)–C(320)	115 (1)
P(3)–Ir(2)–C(2)	100 (1)	Ir(1)–C(1)–O(1)	165 (2)
Ir(1)–P(1)–C(110)	112.2 (9)	Ir(2)–C(2)–O(2)	160 (5)

^aNumbers in parentheses are estimated standard deviations in the least significant digits. A complete listing is provided in the supplementary material.²²

**Figure 6.** ORTEP drawing of **4** showing the atom-numbering scheme.

slightly longer than a normal Ir–Ir single bond (ca. 2.7–2.8 Å) although it is still within the upper limit that is normally considered an Ir–Ir bond (ca. 3.2 Å).

Since the complex is diamagnetic, the Ir₂(μ -H) unit can be considered either as a 3c–2e interaction or a hydride bridging an Ir–Ir single bond. The μ -*t*-Bu₂P group bridges in a symmetrical fashion with Ir(1)–P(3) and Ir(2)–P(3) bond distances of 2.285 (4) and 2.303 (5) Å, respectively. These distances fall within the normal range of values for Ir–P(bridging phosphido) lengths. The Ir–P(phosphine) distances are also normal (Ir(1)–P(1) = 2.342 (7) Å, Ir(2)–P(2) = 2.346 (7) Å). The geometry about each Ir atom is essentially planar, and the dihedral angle between the two planes Ir(1)–P(1)–C(1)–P(3) and Ir(2)–P(2)–C(2)–P(3) is 7.5°.

Reaction of **4 with H₂. Preparation of [Ir(*t*-Bu₂PH)(CO)(μ -H)]₂(H)(μ -*t*-Bu₂P) (**5**).** Interaction of [Ir(CO)(*t*-Bu₂PH)]₂(μ -H)(μ -*t*-Bu₂P) with H₂ (1 atm) in hexane results in an equilibrium mixture of products from which complex **5** may be obtained as yellow crystals in 68% yield. **5** has been characterized spectroscopically and the structure determined by a single-crystal X-ray diffraction study. The other species produced from this reaction

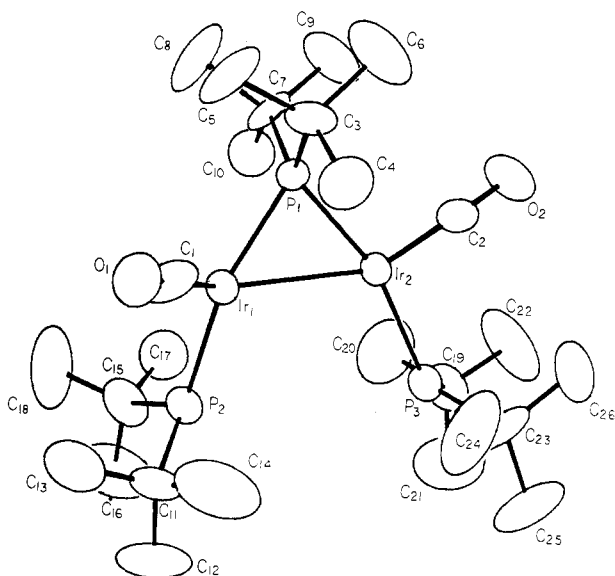


Figure 7. General view of **5** showing the atom-numbering scheme.

Table X. Atomic Positional Parameters for **5**

atom	x	y	z	B, ^a Å ²
Ir(1)	0.16757 (7)	0.09845 (8)	0.14937 (4)	2.98 (2)
Ir(2)	0.31929 (7)	0.22478 (7)	0.09251 (4)	3.02 (2)
P(1)	0.3548 (4)	0.0764 (5)	0.1508 (2)	2.8 (1)
P(2)	0.0014 (5)	0.1889 (5)	0.1485 (3)	3.4 (1)
P(3)	0.2319 (5)	0.3634 (5)	0.0416 (3)	3.4 (1)
O(1)	0.907 (2)	0.372 (2)	0.3856 (8)	5.6 (5)
O(2)	0.544 (1)	0.291 (2)	0.068 (1)	10.0 (7)
C(1)	0.121 (2)	-0.043 (2)	0.129 (1)	4.5 (5)
C(2)	0.454 (2)	0.267 (2)	0.077 (1)	5.3 (6)
C(3)	0.409 (2)	-0.047 (2)	0.113 (1)	3.8 (5)
C(4)	0.352 (2)	-0.048 (3)	0.050 (1)	6.1 (7)
C(5)	0.384 (3)	-0.158 (2)	0.146 (1)	7.5 (9)
C(6)	0.533 (2)	-0.033 (3)	0.104 (1)	7.1 (8)
C(7)	0.428 (2)	0.105 (2)	0.2242 (9)	4.2 (5)
C(8)	0.423 (3)	-0.001 (3)	0.266 (1)	8 (1)
C(9)	0.548 (2)	0.134 (3)	0.217 (1)	7.1 (8)
C(10)	0.379 (2)	0.196 (3)	0.255 (1)	6.3 (7) ^b
C(11)	-0.113 (2)	0.134 (2)	0.102 (1)	5.0 (6)
C(12)	-0.204 (2)	0.211 (3)	0.091 (1)	8.5 (9)
C(13)	-0.156 (2)	0.024 (3)	0.128 (2)	8 (1)
C(14)	-0.069 (3)	0.110 (3)	0.042 (1)	10.1 (9)
C(15)	-0.045 (2)	0.238 (2)	0.221 (1)	5.2 (6)
C(16)	-0.141 (3)	0.309 (3)	0.220 (2)	11 (1)
C(17)	0.050 (3)	0.306 (3)	0.250 (1)	7.3 (8) ^b
C(18)	-0.066 (3)	0.137 (4)	0.262 (1)	11 (1)
C(19)	0.260 (2)	0.502 (2)	0.071 (1)	4.8 (6)
C(20)	0.258 (4)	0.490 (2)	0.137 (2)	9 (1)
C(21)	0.170 (3)	0.587 (3)	0.053 (2)	10 (1)
C(22)	0.373 (2)	0.540 (3)	0.058 (2)	10 (1)
C(23)	0.234 (2)	0.356 (2)	-0.042 (1)	5.0 (6)
C(24)	0.190 (4)	0.245 (3)	-0.057 (1)	10 (1)
C(25)	0.165 (3)	0.440 (3)	-0.075 (1)	9 (1)
C(26)	0.354 (3)	0.364 (4)	-0.060 (1)	9 (1)

^a See footnote *b* in Table II. ^b *B* values for isotropically refined atoms.

appear to be hydrido complexes (by ¹H NMR); however, they have not, so far, been completely identified.

Figure 7 shows the molecular geometry and atom-numbering scheme of complex **5**, while atomic positional parameters and selected bond lengths and angles are given in Tables X and XI. The molecular geometry of **5** consists of a nearly planar arrangement of two Ir and three P atoms, similar to that of **4**. However, the Ir–Ir single bond is now bridged by a *μ*-*t*-Bu₂P unit and two *μ*-hydrido ligands. The position of the hydride ligands in **5** could not be located in the X-ray structure, and the most likely geometry (Scheme I) is based on the heavy-atom positions and NMR spectral data. The ¹H NMR spectrum of **5** contains two

Table XI. Key Bond Distances (Å) and Angles (deg) for **5**^a

Ir(1)–Ir(2)	2.794 (1)	P(1)–C(3)	1.888 (9)
Ir(1)–P(1)	2.325 (2)	P(1)–C(7)	1.882 (9)
Ir(1)–P(2)	2.333 (2)	P(2)–C(11)	1.85 (1)
Ir(1)–C(1)	1.89 (1)	P(2)–C(15)	1.86 (1)
Ir(2)–P(1)	2.283 (2)	P(3)–C(19)	1.86 (1)
Ir(2)–P(3)	2.298 (3)	P(3)–C(23)	1.89 (1)
Ir(2)–C(2)	1.79 (1)	O(2)–C(2)	1.18 (1)
P(1)–Ir(1)	2.325 (2)		
Ir(2)–Ir(1)–P(1)	51.98 (6)	C(3)–P(1)–C(7)	112.7 (5)
Ir(2)–Ir(1)–P(2)	109.78 (7)	C(11)–P(2)–C(15)	111.5 (5)
Ir(2)–Ir(1)–C(1)	127.5 (4)	C(19)–P(3)–C(23)	112.5 (5)
P(1)–Ir(1)–P(2)	158.17 (9)	Ir(2)–C(2)–O(2)	177 (1)
P(1)–Ir(1)–C(1)	100.8 (4)	Ir(1)–P(1)–Ir(2)	74.65 (7)
P(2)–Ir(1)–C(1)	100.5 (3)	Ir(1)–P(1)–C(3)	117.5 (3)
Ir(1)–Ir(2)–P(1)	53.37 (6)	Ir(1)–P(1)–C(7)	115.2 (4)
Ir(1)–Ir(2)–P(3)	109.57 (6)	Ir(2)–P(1)–C(3)	116.4 (3)
Ir(1)–Ir(2)–C(2)	154.2 (3)	Ir(2)–P(1)–C(7)	115.5 (3)
P(1)–Ir(2)–P(3)	162.93 (8)	C(3)–P(1)–C(7)	112.7 (5)
P(1)–Ir(2)–C(2)	101.0 (4)	Ir(1)–P(2)–C(11)	118.4 (4)
P(3)–Ir(2)–C(2)	96.0 (4)	Ir(1)–P(2)–C(15)	116.8 (4)
Ir(2)–P(3)–C(23)	115.9 (4)	C(11)–P(2)–C(15)	111.5 (5)
C(19)–P(3)–C(23)	112.5 (5)	Ir(2)–P(3)–C(19)	115.6 (4)

^a Numbers in parentheses are estimated standard deviations in the least significant digits. A complete listing is provided as supplementary material.²²

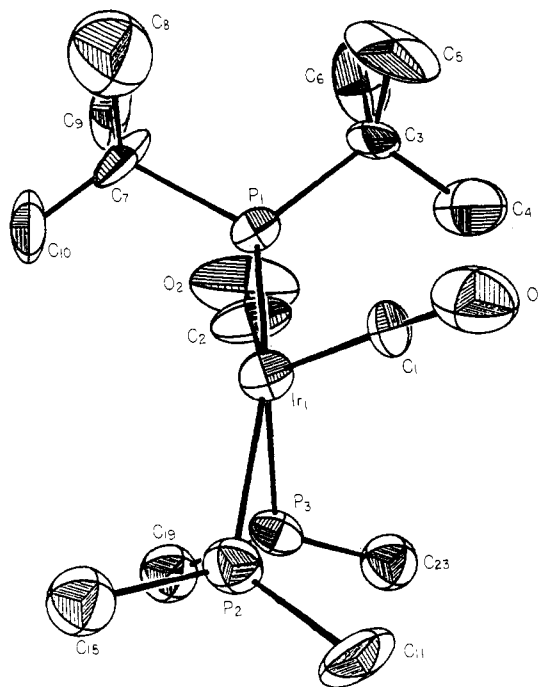


Figure 8. View of **5** taken down the Ir–Ir vector and showing the displacement of the C(1)–O(1) carbonyl group.

multiplets assigned to bridging and terminal hydrides (δ –12.12 (2 H, μ -H), –13.56 (1 H, terminal H)). The heavy-atom framework of **5** is similar to that of **4** except that one CO unit (C(1)–O(1)) attached to Ir(1) is now well out of the Ir₂P₃ plane (Figure 8). A reasonable configuration for the molecule has two bridging H atoms and one terminal H on Ir(1). This would give Ir(1) a roughly octahedral coordination geometry (formally Ir(III), 18e) and Ir(2) would have a trigonal-bipyramidal geometry (Ir(I) 16e).

The key structural parameters of the molecule fall within normal limits. The Ir–Ir single-bond distance of 2.794 (1) Å, and the Ir– μ -P distances, Ir(1)–P(1) = 2.325 (2) Å and Ir(2)–P(1) = 2.283 (2) Å, are comparable to those found in **4**, as well as other iridium phosphido complexes.¹⁰ The iridium–phosphine distances, Ir(1)–P(2) = 2.333 (2) Å and Ir(2)–P(3) = 2.298 (3) Å, are also typical of those found in numerous Ir complexes with coordinated phosphines.

As noted above, ^1H NMR spectra of **5** invariably contained other minor signals in the hydride region. These signals were not completely reproducible, and we assume that they are due to other isomers or impurities. The formation of **5** from **4** is readily reversible, both in the solid state and in solution. Thus crystalline **5**, when not under an atmosphere of H_2 , slowly reverts to **4**, and the process is more rapid under vacuum. Likewise, in solution, **5** is only stable under an atmosphere of H_2 . Exposure of a solution to a nitrogen flush or vacuum results in its rapid conversion to **4**. One explanation for the nonreproducible hydride signals in the ^1H NMR of **5** is that they are due to species resulting from partial loss of hydrogen.

In light of the recent discoveries of dihydrogen ($\eta^2\text{-H}_2$) complexes and the facile reversible addition of H_2 in **4**, we considered the possibility that **5** could contain an $\eta^2\text{-H}_2$ unit. However, all of the hydride signals in the ^1H NMR have T_1 's on the order of 500 ms, which indicates the absence of $\eta^2\text{-H}_2$ groups.¹⁷

Reaction of 4 with CO. Preparation of $(t\text{-Bu}_2\text{PH})(\text{CO})\text{Ir}(\mu\text{-H})(\mu\text{-}t\text{-Bu}_2\text{P})\text{Ir}(\text{CO})_2$ (6**).** **4** reacts with CO (1 atm) in hexane to replace one $t\text{-Bu}_2\text{PH}$ ligand and give $(t\text{-Bu}_2\text{PH})(\text{CO})\text{Ir}(\mu\text{-H})(\mu\text{-}t\text{-Bu}_2\text{P})\text{Ir}(\text{CO})_2$ (**6**) in high yield. The structure of **6** is assigned on the basis of spectroscopic evidence. (See Experimental Section.) Thus, the IR spectrum contains only terminal ν_{CO} absorptions in addition to a weak $\nu_{\text{P-H}}$ peak at 2240 cm^{-1} .

The ^1H NMR spectrum contains signals assigned to the $t\text{-Bu}_2\text{PH}$ and $\text{Ir}(\mu\text{-H})\text{Ir}$ protons (δ 5.31 (d), $^1J_{\text{P-H}} = 358\text{ Hz}$, δ -12.94 (dd), $^2J_{\text{P-H}} = 13, 18\text{ Hz}$), respectively. The $^{31}\text{P}\{^1\text{H}\}$ NMR spectrum consists of two doublets (δ 213.0, 22.9, $^2J_{\text{P-P}} = 133\text{ Hz}$) assigned to the $\mu\text{-}t\text{-Bu}_2\text{P}$ and $t\text{-Bu}_2\text{PH}$ phosphorus nuclei, respectively.

Experimental Section

All reactions were performed under oxygen-free nitrogen or under vacuum. Microanalyses were by the Schwarzkopf Microanalytical Laboratory, Woodside, NY. Hexane, tetrahydrofuran (THF), and toluene were dried over sodium and distilled from sodium/benzophenone under nitrogen before use. Instruments: IR, Perkin-Elmer 1330; NMR, Varian EM-390 (^1H , 90 MHz), FT-80 (^{31}P , 32.384 MHz), Nicolet NT 360 (^1H , ^{31}P), GE QE-300. IR spectra were run as Nujol mulls using KBr plates or KBr disks, or in solution (matched KBr cells). NMR spectra were recorded in C_6D_6 at ambient temperature unless otherwise stated and are in ppm referenced to Me_4Si (δ 0.0, ^1H) and 85% $\text{H}_3\text{PO}_4(\text{aq})$ (δ 0.0, ^{31}P). Melting points were in sealed capillaries under nitrogen (1 atm) and are uncorrected. Iridium carbonyl chloride ($\text{Ir}(\text{CO})_3\text{Cl}$)_n and $\text{Ir}_4(\text{CO})_{12}$ were purchased from the Strem Chemical Co., Newburyport, MA, and were used as received. $t\text{-Bu}_2\text{PH}$,^{18a} $t\text{-Bu}_2\text{AsH}$,^{18b} and $\text{Li-}t\text{-Bu}_2\text{P}$ ¹⁹ were prepared as previously described.

$[\text{Ir}(\mu\text{-}t\text{-Bu}_2\text{P})(\text{CO})_2]_2$ (1**).** $\text{Li-}t\text{-Bu}_2\text{P}$ (1.15 mL of a 1.4 M THF solution, 1.6 mmol) was added dropwise to a suspension of $[\text{Ir}(\text{CO})_3\text{Cl}]_n$ (0.50 g, 0.80 mmol) in hexane (30 mL) at -100°C . The mixture was allowed to warm to room temperature over a period of 5 h during which time the solution darkened. The mixture was stirred at room temperature (2 h), and volatile materials were removed under vacuum. The residue was extracted with hexane ($2 \times 20\text{ mL}$) and the resulting solution passed down an alumina column ($5\text{ cm} \times 5\text{ cm}$). The deep red solution was collected and concentrated under vacuum (ca. 5 mL). Cooling (-40°C) for 12 h yielded very dark red crystals, which were collected and dried under vacuum: yield 0.22 g (35%); mp $256\text{--}260^\circ\text{C}$ dec. NMR: ^1H (90 MHz), δ 1.18 (m, $t\text{-Bu}_2\text{P}$); $^{31}\text{P}\{^1\text{H}\}$ (32.384 MHz) δ 262.51 (s, $t\text{-Bu}_2\text{P}$). IR: (hexane solution) 1960 s, 1935 s cm^{-1} ; (KBr disk) 1995 s, 1955 vs, br, 1920 w cm^{-1} . Anal. Calcd for $\text{C}_{20}\text{H}_{36}\text{Ir}_2\text{O}_4\text{P}_2$: C, 30.53; H, 4.58; P, 7.88. Found: C, 30.55; H, 4.81; P, 7.52.

$[\text{Ir}(\mu\text{-Bu}_2\text{As})(\text{CO})_2]_2$ (2**) and $\text{Ir}_4(\mu\text{-}t\text{-Bu}_2\text{As})_4(\mu\text{-CO})_2(\text{CO})_2$.** Dry toluene (40 mL) and di-*tert*-butylarsine (0.15 mL, 0.15 g, 0.79 mmol) were added to tetrairidium dodecacarbonyl (0.204 g, 0.185 mmol), and the resulting mixture was refluxed for 12 h, during which time the solution gradually turned black. The solution was then allowed to cool to

room temperature, filtered, and concentrated under vacuum until a precipitate began to form (ca. 35 mL). Cooling (-5°C) resulted in the formation of black crystals of $\text{Ir}_4(\mu\text{-}t\text{-Bu}_2\text{As})_4(\text{CO})_4$ (yield 0.13 g, 43%). The mother liquor was removed via cannula and evaporated to dryness under vacuum. The residue was extracted with dry hexane (20 mL) to give a yellow-black solution, which was filtered, concentrated, and cooled to give yellow crystals of $[\text{Ir}(\mu\text{-}t\text{-Bu}_2\text{As})(\text{CO})_2]_2$ (**2**). They were collected and dried under vacuum: yield 0.04 g (12%); mp $280\text{--}286^\circ\text{C}$ dec. ^1H NMR (300 MHz) (C_6D_6): δ 1.44 (s, $t\text{-Bu}_2\text{As}$). IR (KBr disk): 2990–2820 br, m, 2010 vs, 1972 vs, 1451 m, 1375 w, 1352 w, 1251 s, 1148 m, 1080 br, s, 1006 br, s, 790 s, 569 m, 502 m, 393 br, m cm^{-1} . Anal. Calcd for $\text{C}_{20}\text{H}_{36}\text{As}_2\text{Ir}_2\text{O}_4$: C, 27.46; H, 4.15. Found: C, 27.69; H, 4.33. Details of $\text{Ir}_4(\mu\text{-}t\text{-Bu}_2\text{As})_4(\mu\text{-CO})_2(\text{CO})_2$ have been reported elsewhere.¹⁰

$\text{Ir}_3(\text{CO})_5(\mu\text{-}t\text{-Bu}_2\text{P})_3$ (3**) and $[\text{Ir}(\text{CO})(t\text{-Bu}_2\text{PH})]_2(\mu\text{-H})(\mu\text{-}t\text{-Bu}_2\text{P})$ (**4**).** $t\text{-Bu}_2\text{PH}$ (0.73 mL, 5.3 mmol) was added to a suspension of $\text{Ir}_4(\text{CO})_{12}$ (0.98 g, 0.89 mmol) in toluene (80 mL). The mixture was heated under reflux (12 h) during which time all the material dissolved, forming a dark red solution. Volatile materials were removed under vacuum, and the residue was extracted into hexane ($3 \times 30\text{ mL}$). The filtered combined extracts were reduced in volume under vacuum (ca. 15 mL) and cooled (-35°C), producing a mixture of black air-stable crystals of **3** and orange-red solvent-dependent, air-sensitive crystals of **4**. They were collected, dried under vacuum, and separated manually in a drybox. Crystals of **3** and **4** can also be separated by fractional crystallization from hexane (-20°C) since compound **3** crystallizes first. **3**: yield 0.33 g (24% based on Ir); mp $313\text{--}315^\circ\text{C}$ dec. IR: (THF solution, KBr cells) 2010 s, 1990 m, 1972 m, 1947 s, 1936 s cm^{-1} ; (Nujol mull, NaCl plates) 2010 s, 1985 s, 1974 s, 1942 s, 1931 s, 1373 m, 1361 s, 1166 m, 1018 w, 1011 w, 937 w, 806 m cm^{-1} . ^1H NMR (361.084 MHz): δ 1.37 (br m, $\mu\text{-}t\text{-Bu}_2\text{P}$). $^{31}\text{P}\{^1\text{H}\}$ NMR (toluene- d_6): at 25°C , δ 306.0 (br s), 184.0 (br s); at -25°C , δ 304.9 (d), 184.0 (t, $^2J_{\text{P-P}} = 72\text{ Hz}$, $\mu\text{-}t\text{-Bu}_2\text{P}$). Anal. Calcd for $\text{C}_{29}\text{H}_{54}\text{Ir}_3\text{O}_3\text{P}_3$: C, 30.23; H, 4.72; P, 8.06. Found: C, 30.17; H, 4.85; P, 7.91. **4**: yield 0.81 g (52% based on Ir); mp $175\text{--}180^\circ\text{C}$ dec. IR: (hexane solution, KBr cells) 2305 w, 2020 w, 1953 s, 1948 s, 1940 s cm^{-1} ; (Nujol mull, NaCl plates) 2300 w, 1938 br s, 1910 sh, 1363 m, 1178 m, 1020 m, 811 m cm^{-1} . ^1H NMR (361.084 MHz): δ 5.24 (d, 2 H, $^1J_{\text{P-H}} = 322\text{ Hz}$, $t\text{-Bu}_2\text{PH}$), 1.58 (d, 18 H, $^3J_{\text{t-Bu-P}} = 17\text{ Hz}$, $\mu\text{-}t\text{-Bu}_2\text{P}$), 1.21 (d, 36 H, $^3J_{\text{t-Bu-P}} = 17\text{ Hz}$, $t\text{-Bu}_2\text{PH}$), -6.76 (m, 1 H, $\mu\text{-H}$). $^{31}\text{P}\{^1\text{H}\}$ NMR (32.384 MHz): δ 193.8 (t, $\mu\text{-}t\text{-Bu}_2\text{P}$), 44.6 (d, $^2J_{\text{P-P}} = 183\text{ Hz}$, $t\text{-Bu}_2\text{PH}$). Anal. Calcd for $\text{C}_{32}\text{H}_{77}\text{Ir}_2\text{O}_2\text{P}_3$: C, 39.82; H, 7.41; P, 9.63. Found: C, 39.95; H, 7.62; P, 9.43.

$[\text{Ir}(t\text{-Bu}_2\text{PH})(\text{CO})(\mu\text{-H})]_2(\mu\text{-}t\text{-Bu}_2\text{P})$ (5**).** A concentrated solution of $[\text{Ir}(t\text{-Bu}_2\text{PH})(\text{CO})]_2(\mu\text{-H})(\mu\text{-}t\text{-Bu}_2\text{P})$ (**4**) (0.23 g, 0.26 mmol) in hexane (15 mL) at room temperature was placed under vacuum until the solvent began to boil. The solution was then exposed to H_2 (1 atm). The solution was allowed to react for 15 min during which time it turned from red-orange to yellow. The solution was cooled (-35°C), producing yellow, air-sensitive, H_2 -dependent crystals of **5**. They were collected, dried under a stream of H_2 , and stored under H_2 (1 atm): yield (isolated) 0.15 g (68% based on Ir). IR (Nujol mull, NaCl plates): 2310 w, 2300 w, 2070 w, br, 1978 m, br, 1915 s, 1362 m, 1260 w, 1176 m, 1021 m, 896 w, 864 w, 839 w, 809 m cm^{-1} . ^1H NMR (361.084 MHz): δ 5.38 (d, 1 H, $J_{\text{H-P}} = 314\text{ Hz}$, $t\text{-Bu}_2\text{PH}$), 4.93 (d, 1 H, $J_{\text{H-P}} = 331\text{ Hz}$, $t\text{-Bu}_2\text{PH}$), 1.54 (d, 18 H, $J_{\text{t-Bu-P}} = 14\text{ Hz}$, $\mu\text{-}t\text{-Bu}_2\text{P}$), 1.33 (d, 18 H, $J_{\text{H-P}} = 14\text{ Hz}$, $t\text{-Bu}_2\text{PH}$), 1.22 (d, 18 H, $J_{\text{P-H}} = 14\text{ Hz}$, $t\text{-Bu}_2\text{PH}$), -12.12 (br quar, 2 H, $\mu\text{-H}$), -13.56 (br t, 1 H, $\mu\text{-H}$). $^{31}\text{P}\{^1\text{H}\}$ NMR (32.384 MHz): δ 155.1 (dd, $^2J_{\text{P(1)-P(2)}} = 200\text{ Hz}$, $^2J_{\text{P(1)-P(3)}} = 181\text{ Hz}$, $\mu\text{-}t\text{-Bu}_2\text{P}$), 44.2 (dd, $^2J_{\text{P(2)-P(1)}} = 200\text{ Hz}$, $^3J_{\text{P(2)-P(3)}} = 4\text{ Hz}$, $t\text{-Bu}_2\text{PH}$), 27.1 (dd, $^2J_{\text{P(3)-P(1)}} = 181\text{ Hz}$, $^3J_{\text{P(3)-P(2)}} = 4\text{ Hz}$, $t\text{-Bu}_2\text{PH}$). Anal. Calcd for $\text{C}_{26}\text{H}_{59}\text{Ir}_2\text{O}_2\text{P}_3$: C, 35.44; H, 6.75; P, 10.55. Found: C, 35.67; H, 6.89; P, 10.27.

Synthesis of $(t\text{-Bu}_2\text{PH})(\text{CO})\text{Ir}(\mu\text{-H})(\mu\text{-}t\text{-Bu}_2\text{P})\text{Ir}(\text{CO})_2$ (6**).** A concentrated solution of **4** (0.20 g, 0.23 mmol) in hexane (10 mL) was placed under an atmosphere of CO (1 atm) and stirred with the aid of a magnetic follower. The color of the solution rapidly changed from red to yellow. The solution was cooled (-40°C), producing yellow crystals of **6**. They were collected and dried under vacuum. The mother liquor was reduced in volume under vacuum, placed under a CO atmosphere, and cooled to yield more crystals of **6**: yield 0.12 g (71% based on Ir). IR: (THF solution, KBr cells) 2240 w, 2030 s, 2015 s, 1992 br, s, 1965 sh, m, 1933 m, 1891 m cm^{-1} ; (Nujol mull, NaCl plates) 2033 s, 2008 m, 1991 br, s, 1960 sh, w, 1932 s, 1886 s, 1260 m, 1165 br, m, 1014 w, 860 m cm^{-1} . ^1H NMR (361.084 MHz): δ 5.31 (d, 1 H, $^1J_{\text{P-H}} = 358\text{ Hz}$, $t\text{-Bu}_2\text{PH}$), 1.38 (d, 18 H, $J_{\text{P-H}} = 15\text{ Hz}$, $\mu\text{-}t\text{-Bu}_2\text{P}$), 1.06 (d, 18 H, $J_{\text{P-H}} = 15\text{ Hz}$, $t\text{-Bu}_2\text{PH}$), -12.94 (dd, 1 H, $J_{\text{P-H}} = 13, 18\text{ Hz}$, $\mu\text{-H}$). $^{31}\text{P}\{^1\text{H}\}$ NMR (32.384 MHz): δ 213 (d, $^2J_{\text{P-P}} = 133\text{ Hz}$, $\mu\text{-}t\text{-Bu}_2\text{P}$), 22.9 (d, $^2J_{\text{P-P}} = 133\text{ Hz}$, $\text{HP}(t\text{-Bu}_2)$). Anal. Calcd for $\text{C}_{19}\text{H}_{38}\text{Ir}_2\text{O}_3\text{P}_2$: C, 29.99; H, 5.03; P, 8.14. Found: C, 30.18; H, 5.31; P, 8.02.

X-ray Crystal Structure Determinations. Details of crystal data and a summary of intensity data collection parameters for **1–5** are given in

- (17) (a) Kubas, G. J.; Ryan, R. R.; Swanson, B. I.; Vergamini, P. J.; Wasserman, J. J. *J. Am. Chem. Soc.* **1984**, *106*, 451–452. (b) Wasserman, H. J.; Kubas, G. J.; Ryan, R. R. *J. Am. Chem. Soc.* **1986**, *108*, 2294–2301. See also: Crabtree, R. H.; Lavin, M.; Bennevoit, L. *J. Am. Chem. Soc.* **1986**, *108*, 4032–4037 and references therein.
(18) (a) Hoffman, H.; Schellenbeck, P. *Chem. Ber.* **1966**, *99*, 1134. (b) Tzschach, A.; Deylig, W. Z. *Anorg. Allg. Chem.* **1956**, *336*, 36.
(19) Issleib, K.; Krech, F. *J. Organomet. Chem.* **1968**, *13*, 283.

Table I. Data were collected on an Enraf-Nonius CAD-4 diffractometer at 23 ± 2 °C using graphite-monochromated Mo K α radiation. Details of the standard data collection methods were similar to those outlined in ref 4. All calculations were performed on a PDP 11/44 computer using the Enraf-Nonius software package SDP PLUS.²⁰ Lattice parameters were determined from 25 strong reflections collected by the $\theta/2\theta$ scan technique (program SEARCH, 2 θ values in Table I). For each structure, the data were corrected for Lorentz and polarization effects. The structures were solved by direct methods (MULTAN)²¹ and successive cycles of difference Fourier maps followed by least-squares refinement. Supplementary material for all structures is available.²²

1. Crystals were grown from hexane solutions (-20 °C) and mounted in thin-walled glass capillaries under nitrogen. Systematic absences indicated a choice of either *Pnmm* or *Pnn2* as the space group. *Pnmm* was chosen as the correct one on the basis of successful refinement. An empirical absorption correction (ψ scan) was applied (program EAC). Unit weights were used in the initial cycles of least-squares refinement. In the final stages of refinement, a weighting scheme with a non-Poisson contribution and an ignorance factor of $P = 0.06$ was employed.²³ Hydrogen atoms were either located directly or placed in idealized positions (sp³ geometry, C-H = 0.95 Å) and refined positionally but not thermally. Final full-matrix least-squares refinement with anisotropic thermal parameters for all non-hydrogen atoms gave final values of $R = 0.0301$ and $R_w = 0.0382$ where $R = \sum |F_o| - |F_c| / \sum |F_o|$ and $R_w = [\sum w(|F_o| - |F_c|)^2 / \sum w(|F_o|)^2]^{1/2}$. The function minimized in the least-squares refinement was $\sum w(|F_o| - |F_c|)^2$, $w = 1/\sigma^2(|F_o|)$.

2. Examination of the diffraction symmetry and the systematic absences hkl , $h + k = 2n + 1$, indicated a choice of the monoclinic space groups *C2*, *Cm*, or *C2/m*. The space group *C2/m* (No. 12) was chosen to be the correct one on the basis of successful refinement of the structure. The check reflections showed no decrease in intensity over the course of data collection, and hence no correction was applied. A ψ scan of three reflections having χ values between 80 and 90° showed a minimum percent transmission of 16.44 and a maximum percent transmission of 99.60. An empirical absorption correction was applied. The observed structure factors of equivalent reflections were averaged, with agreement factors of 0.034 on intensity and 0.019 on F_o . Hydrogen atoms were not located. Data with intensities less than $3\sigma(I)$ and $(\sin \sigma)/\lambda$ less than 0.1 were excluded, and a non-Poisson contribution weighting scheme with an experimental instability factor of $P = 0.06$ was used in the final stages of refinement. The atoms were refined to the final R values shown in Table I. The maximum peak in the final difference Fourier map had a height of 0.956 e/Å³ and was located 0.815 Å from the iridium.

3. The space group was uniquely determined by systematic absences to be *P2₁/c*. Due to poor crystal quality, there was insufficient data to refine all non-hydrogen atoms anisotropically since there was very little useful data beyond $2\theta = 36^\circ$. Therefore, the Ir and P atoms were refined anisotropically while the C and O atoms were refined isotropically.

4. The crystal structure determination was complicated by several factors, the main one being poor crystal quality. The crystals were fragile and disintegrated immediately in the absence of solvent. After a number of attempts, a thin platelike crystal (0.10 × 0.40 × 0.80 mm) was mounted under a hexane-saturated nitrogen atmosphere and was found to be suitable for data collection. The space group was uniquely determined by systematic absences as *P2₁2₁2₁*. The decrease in intensity of the standard reflections was 5.8%; therefore, an anisotropic decay correction was applied. There was a severe problem with absorption due to the presence of iridium and the relative thinness of the crystal in one dimension. Transmission values in the ψ scan ranged from 22% to 99%, and so an empirical absorption correction (ψ scan) was applied.

Two of the methyl carbons in the *tert*-butyl groups on P(1) were not located. Attempts to generate the positions of the two missing carbon atoms were made, but they did not refine successfully, so they have been omitted from the final tables. A difference Fourier map revealed the presence of peaks corresponding to a hexane of crystallization. These peaks were assigned multiplicities of 0.5 and isotropic temperature factors of 6.0 and were used in the structure factor calculation but were not refined. In the final difference Fourier, there were seven peaks greater than 1 e Å⁻³ (the highest was 1.44 e Å⁻³), all of which were less than 1.5 Å from the iridium atoms. Assignment of the correct enantiomorph was equivocal because of the large absorption problem.

5. Crystals suitable for X-ray diffraction were grown by cooling a toluene solution (-35 °C). The crystals were mounted in thin-walled glass capillaries and sealed under hydrogen. The monoclinic space group *P2₁/c* (No. 14) was uniquely determined by the systematic absences $h0l$, $l = 2n + 1$, and $0k0$, $k = 2n + 1$. Data were collected in the $\pm h, +k, +l$ quadrant between 2θ values of 3 and 48°. The check reflections indicated <1% decrease in intensity over the course of data collection, and hence no decay correction was applied. A ψ scan of four reflections having χ values between 80 and 90° showed a minimum percent transmission of 64.1 and a maximum percent transmission of 99.9. An empirical absorption correction was applied. The observed structure factors of equivalent reflections were averaged, with agreement factors of 0.048 for intensity and 0.086 on F_o . Hydrogen atoms were not located. Data with intensities less than $3\sigma(I)$ were excluded, and a non-Poisson contribution weighting scheme with an experimental instability factor of $P = 0.05$ was used in the final stages of refinement.²³ The atoms were refined to the final R values shown in Table I. The maximum peak in the final difference Fourier map had a height of 1.441 e/Å³ and was located 1.283 Å from Ir(1).

Acknowledgment. We thank the Robert A. Welch Foundation (Grant F-816), the National Science Foundation (Grant CHE8517759), and the Texas Advanced Technology Research Program for support. We also thank Johnson Matthey Inc. for a loan of RhCl₃·xH₂O. R.A.J. thanks the Alfred P. Sloan Foundation for a fellowship (1985-1987).

Registry No. 1, 110613-91-7; 2, 101078-39-1; 3, 110613-92-8; 4-C₆H₁₄, 110637-25-7; 5, 110613-93-9; 6, 110613-94-0; [Ir(CO)₃Cl]_n, 28700-98-3; Ir₄(μ -*t*-Bu₂As)₄(μ -CO)₂(CO)₂, 101078-38-0; Ir₄(CO)₁₂, 18827-81-1; Ir, 7439-88-5.

Supplementary Material Available: Complete listings of bond lengths and bond angles for 1 and 3-5, anisotropic thermal parameters for 1-5, isotropic thermal parameters for 3, and hydrogen atom parameters for 1 (17 pages); listings of observed and calculated structure factors for 1-5 (84 pages). Ordering information is given on any current masthead page.

(20) B. A. Frenz and Associates, College Station TX 77840, 4th ed., 1981.

(21) Germain, G.; Main, P.; Wolfson, M. M. *Acta Crystallogr., Sect. A: Cryst. Phys., Diffraction, Theor. Gen. Crystallogr.* 1971, **A27**, 368.

(22) See paragraph at end of paper regarding supplementary material.

(23) P is used in the calculation of $\sigma(I)$ to downweight intense reflections in the least-squares refinement. The function minimized was $\sum w(|F_o| - |F_c|)^2$, where $w = 4(|F_o|)^2 / [\sum (|F_o|)^2]^2$, where $[\sum (|F_o|)^2]^2 = [\sum^2 (C - R^2B) + (P(|F_o|)^2)^2] / Lp^2$, where S^2 is the scan rate squared, C is the total background count, R^2 is the ratio squared of scan time to background count, and Lp is the Lorentz polarization factor.